Talanta 85 (2011) 2113–2120

Contents lists available at ScienceDirect

Talanta

journal homepage: www.elsevier.com/locate/talanta

Aptamer-quantum dots conjugates-based ultrasensitive competitive electrochemical cytosensor for the detection of tumor cell

Jingjing Li[a], Mi Xu[a], Haiping Huang[a,c], Jinjun Zhou[a], E.S. Abdel-Halim[b], Jian-Rong Zhang[a], Jun-Jie Zhu[a,*]

[a] State Key Lab of Analytical Chemistry for Life Science, School of Chemistry and Chemical Engineering, Nanjing University, Nanjing 210093, People's Republic of China
[b] Petrochemical Research Chair, Chemistry Department, College of Science, King Saud University, Riyadh 11451, P.O. Box 2455, Kingdom Saudi Arabia
[c] Center for Materials Analysis and Testing, Jiangxi University of Science and Technology, Ganzhou, 341000, People's Republic of China

ARTICLE INFO

Article history:
Received 21 May 2011
Received in revised form 11 July 2011
Accepted 12 July 2011
Available online 21 July 2011

Keywords:
Aptamer
Cancer cell
Electrochemistry
Fluorescence imaging
Quantum dots

ABSTRACT

A novel competitive electrochemical cytosensor was reported by using aptamer (Apt)-quantum dots (Qdots) conjugates as a platform for tumor cell recognition and detection. The complementary DNA (cDNA), aptamer and Qdots could be assembled to the gold electrode surface. When the target cells existed, they could compete with cDNA to bind with Apt-Qdots conjugates based on the specific recognition of aptamer to MUC1 protein overexpressed on the cell surface, which resulted in the denaturation of double-stranded DNA structure and the release of the Apt-Qdots conjugates from the electrode. Electrochemical stripping measurement was then employed to determine the Cd^{2+} concentration in Qdots left at the electrode. The peak current was inversely proportional to the logarithmic value of cell concentration ranging from 1.0×10^2 to 1.0×10^6 cells mL^{-1} with a detection limit of 100 cells mL^{-1}. Meanwhile, the recognition of aptamer to the target cells could be clearly observed through the strong fluorescence from Qdots. This is an example of the combination of aptamer and nanoparticles for the application of cell analysis, which is essential to cancer diagnosis and therapy.

1. Introduction

Cancer is a main cause of the worldwide death and there is an estimated 12 million deaths in 2030 which is learnt from World Health Organization. Thus, early diagnosis and therapy for cancers is of the utmost importance. In recent decades, some electrochemical cytosensors with various detection means, such as electrochemical impedance spectroscopy (EIS), cyclic voltammetry (CV) and open circuit potential (OCP), have been fabricated for cancer cell detection [1–5]. However, the challenge for the fabrication of cytosensors was the weak selectivity for the target cells [6].

Aptamers (Apt) are single-stranded nucleic acid molecules which derived from random single-stranded nucleic acid sequence pools and selected via the process called SELEX (Systematic Evolution of Ligands by Exponential Enrichment) [7–9]. They have shown reduced immunogenecity and toxicity compared to other biological therapeutics, increased thermal stability and reproducibility compared to antibodies, and the possibility of production via solid-phase synthesis. Aptamers possess high affinity and specificity toward a great variety of targets, ranging from metal ions [10,11] and small chemicals [12] to large proteins [13–15] and the whole cells [16,17]. They could fold into specific 3-D conformations after combining with the targets via various acting forces such as hydrogen bonding, electrostatic, and sometimes hydrophobic interactions, etc. [18]. Based on the high selectivity, aptamers and their conjugates with nanoparticles (NPs) are well suited for cellular application, including diagnostics and therapeutics. By using a series of Apt-NPs conjugates as the novel molecular recognition tools, Tan and co-workers have provided a vast platform for specific cells detection by the means of flow cytometric analysis [19] and have already extended the use of Apt-NPs conjugates for the collection and detection of multiple cancer cells [20]. Jong and co-workers developed a class of Apt-NPs that could recognize and therapeutically target cancer cells and demonstrated 3–4 times enhanced growth inhibition efficacy compared with DNA aptamers alone [21].

In recent years, many aptamer-based electrochemical sensors have emerged and are still gaining increasing developments [22–25]. They not only have the advantages of electrochemical sensors, such as rapid response, high sensitivity, ease of use, low cost and small-sized commercial detectors, but also inherit the high affinity and specificity of aptamers. The detection principle is basically based on the aptamer structural changes [26,27] and sandwich structural formation [28]. The methods mainly include electrochemical impedance spectroscopy [29] and

* Corresponding author. Tel.: +86 25 83597204; fax: +86 25 83597204.
E-mail address: jjzhu@nju.edu.cn (J.-J. Zhu).

0039-9140/$ – see front matter © 2011 Elsevier B.V. All rights reserved.
doi:10.1016/j.talanta.2011.07.055

electrochemical stripping [30,31]. The latter have been particularly used for detecting metal-nanoparticle tags, owning to its 'built-in' pre-concentration step in electrodeposition, which leads a remarkable sensitivity [32].

Herein, a competitive electrochemical cytosensor was developed based on electrochemical stripping measurements by using Apt-Qdots conjugates as a platform for tumor cell recognization and detection. Qdots cannot only serve as vehicles for the detection of cells, but also act as tags for cell imaging. The latter can be realized because Qdots have narrow, size-tunable emission spectra and possess a high quantum yield, all of which have rivaled those of organic dyes in many applications [33–35]. Apt-Qdots conjugates have already been widely used in optical area for cancer imaging, therapy, and drug delivery [36–39], but to the best of our knowledge, they have not been applied in electrochemical cytosensor yet. On the other hand, a competitive reaction was introduced for the construction of our cytosensor, which was reported to have the potential to alleviate overdose or drug-induced allergic reactions. Lu et al. have used a complementary DNA of the aptamer as an antidote to disrupt aptamer-mediated targeted drug delivery [40]. And Yu et al. developed an aptasensor based on competitive-binding for human neutrophil elastase detection [41].

For the proof of concept, breast tumor cells (MCF-7 breast cancer cell line), on which MUC1 protein was overexpressed, were used as model target. A 25-base oligonucleotide with specific binding properties ($Kd \sim 0.135$ nM) for MUC1 peptide [42] was chosen to conjugate with Qdots, thus developing a specific platform for detecting and imaging MCF-7 cells. The mucin protein (MUC1) is a large, rod-like glycoprotein consisting of a N-terminus projecting away from the cell surface as a long filament made of tandem repeats, a transmembrane region and a C-terminus cytoplasmatic tail [43,44]. It is widely expressed on normal epithelial tissues. When they become malignant, its expression increased at least 10-fold [45]. So it is a well-known tumor marker in epithelial malignancies and can be used in immunotherapeutic and diagnostic approaches [46]. Till now, a number of MUC1-related modalities have been used in clinical trials, ranging from radiolabeled antibodies to MUC1 peptide vaccines and gene therapies. Since Ferreira et al. [42] reported the selection of DNA aptamers that bound to the MUC1 peptides with high affinity and specificity, a lot of biodistribution studies have been carried out [47]. Recently, Yu et al. proposed a method for the detection of MUC1 based on aptamer with Qdots as the fluorescence signal and the detection limit was as low as 250 nM [48].

The principle of our competitive electrochemical cytosensor used for detecting and imaging of target cells is shown in Scheme 1. 5′-NH_2 aptamer, which can specifically recognize MUC1 on the cell surface, was firstly captured by the thiolated complementary DNA anchored on the gold electrode surface. Then the functional carboxyl groups on the surface of Qdots were activated by 1-ethy-3-(3-dimethylaminopropyl) carbodiimide hydrochloride (EDC) and *N*-hydroxy-succinimide (NHS) to form an intermediate, which could combine with amine-containing aptamers. Since MUC1 protein on the cell surface could compete with cDNA to conjugate with Apt-Qdots conjugates, the number of Qdots retained at the electrode decreased in the presence of target cells. After dissolving the remaining Qdots, the concentration of the obtained metal species was detected by electrochemical stripping, which was correlated to the concentration of target cells in solution.

By using this competitive electrochemical cytosensor, we have successfully detected as low as 100 MCF-7 cells mL^{-1} with a linear calibration range from 1.0×10^2 to 1.0×10^6 cells mL^{-1}. Meanwhile, all of the reactions occurred on the surface of gold electrode and there was no need for extra separation procedure. In addition, with the development of aptamer SELEX technology [49], this method can be easily extended to other cancer cell and analyte determination once related aptamers have been selected.

2. Experimental

2.1. Chemicals

N-Hydroxy-succinimide (NHS), 6-mercapto-1-hexanol (MCH), Tween-20, and bovine serum albumin (BSA, 96–99%) were obtained from Sigma (St. Louis, MO, USA). 1-Ethy-3-(3-dimethylaminopropyl) carbodiimide hydrochloride (EDC) was purchased from Pierce (Rockford, IL). Tellurium powder (Te, 99.8%, 200 mesh) and 3-mercaptopropionic acid (MPA, 99%) were obtained from Acros Organics (New Jersey, USA). Cadmium chloride and potassium borohydride were purchased from Tianjin Chemical Research Institute (Tianjin, China). Disodium hydrogen phosphate, Potassium dihydrogen phosphate, sodium hydroxide, magnesium chloride and sodium chloride were obtained from Nanjing Chemical Reagents Factory (Nanjing, China). All other chemicals were of analytical grade and were used as received. The ultrafiltration filter (Millipore Corp.) was used to separate and concentrate the sample solution. All aqueous solutions were prepared using ultra-pure water (≥18 MΩ, Milli-Q, Millipore).

2.2. Apparatus and characterization

Electrochemical measurements were performed on a CHI 660a workstation (Shanghai Chenhua, Shanghai, China) in a solution of pH 7.4 PBS containing 10 mM $Fe(CN)_6^{3-/4-}$ and 0.1 M KCl with a conventional three-electrode system composed of the modified gold electrode as the working electrode, a platinum wire as the auxiliary and a saturated calomel electrode as the reference. The EIS analyses were carried out on an Autolab PGSTAT12 (Ecochemie, BV, Netherlands) in 10 mM pH 7.4 PBS containing 10 mM $Fe(CN)_6^{3-/4-}$ and 0.1 M KCl with the frequency range of $10^{-1} \sim 10^5$ Hz. UV–vis spectra were recorded on a UV-3600 spectrophotometer (Shimadzu, Kyoto, Japan) and the fluorescence measurements were carried out using a RF-5301PC (Shimadzu, Kyoto, Japan). IR spectra were recorded on a Nicolet 400 Fourier transform infrared (FT-IR) spectrometer (Madison, WI). All experiments were performed at room temperature.

2.3. DNA aptamer synthesis

All probes and DNAs were synthesized by Shanghai Sangon Biotechnology Co. Ltd. (Shanghai, China).

MUC1 binding aptamer: 5′-GCA GTT GAT CCT TTG GAT ACC CTG G-3′

5′-NH_2-modified MUC1 binding aptamer: 5′-NH_2- GCA GTT GAT CCT TTG GAT ACC CTG G-3′

5′-thiol-modified complementary DNA: 5′-thiol-CCA GGG TAT CCA AAG G-3′

2.4. Preparation of MPA-modified CdTe Qdots

The synthesis of water-soluble CdTe quantum dots was referred to the method reported previously [50–52]. Briefly, $CdCl_2 \cdot 2.5H_2O$ (0.0561 g, 0.25 mmol) and MPA (34 μL, 0.39 mM) were added into 195 mL doubly distilled water, and the pH was adjusted to 8.0–8.5 by the addition of a 5% NaOH solution. The solution was heated to 93 °C and then 2.0 mL of freshly prepared KHTe solution produced by the reaction of KBH_4 (0.0480 g, 0.89 mM) with tellurium powder (0.0479 g, 0.375 mM) in a 2.0 mL aqueous solution was injected into the above $CdCl_2$–MPA solution. The resulting mixture solution was refluxed under nitrogen flow at 93 °C for about 5 h to obtain CdTe Qdots with an emission maximum at 620 nm (line a

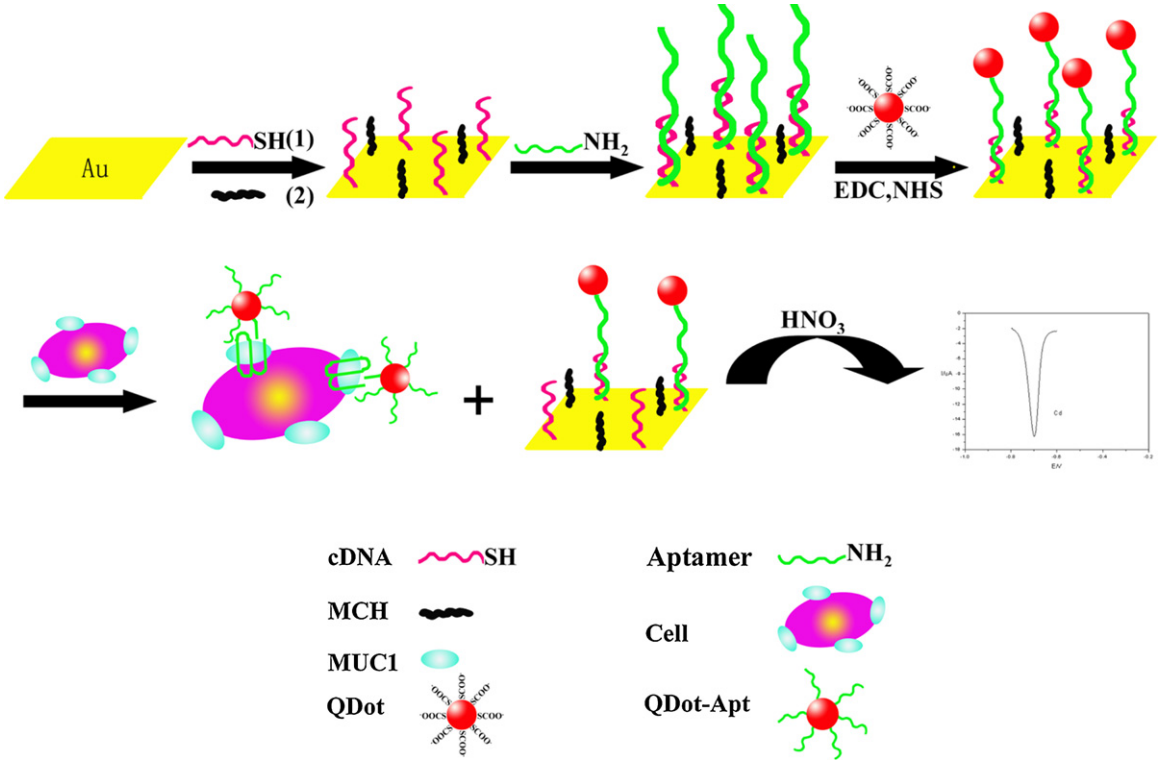

Scheme 1. Fabrication steps for the competitive electrochemical cytosensor.

in Fig. 1) and absorption at 550 nm (line b in Fig. 1). The obtained Qdots solution was further purified by ultrafiltration according to the previous report to remove unreacted MPA [53]. The purified water-soluble Qdots possessed a bright fluorescence and a good stability in a buffer. The concentration of the CdTe Qdots was calculated to be 9 μM according to the equation described previously [54].

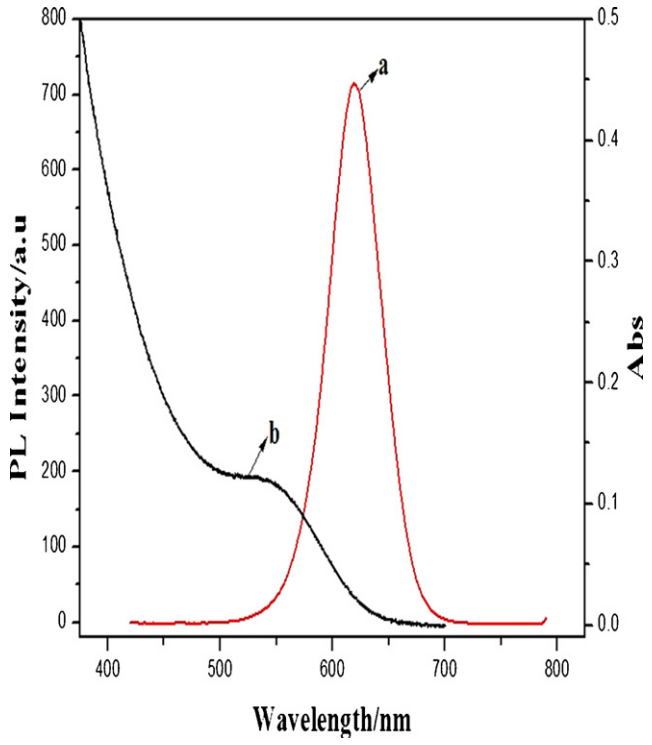

Fig. 1. Photoluminescence and UV–vis absorption spectra of the CdTe Qdots in aqueous solution. Excitation wavelength: 420 nm.

2.5. Synthesis of Apt-Qdots conjugates

Apt-Qdots conjugates were synthesized according to a modified procedure of a literature [36,55]. Carboxyl CdTe Qdots (10 μL, 9 μM) was activated in the presence of 10 μL (4.2 mg mL^{-1}) of EDC and 5 μL (2.1 mg mL^{-1}) of NHS for 15 min. The resulting *N*-hydroxy-succinimide-activated Qdots were covalently linked to 5′-NH_2 modified MUC1 aptamer (45 μL, 5 μM). The reaction was carried out under gentle mixing for 1 hour. Then the Apt-Qdots conjugates were purified by ultrafiltration on 30,000 MW size filter and centrifugation at 3000 rmp for 15 min and washed twice with water to remove nonspecifically bound aptamer. The final Apt-Qdots conjugates were resuspended in buffer solution and stored at 4 °C before use. All the buffer solution used in the experiments was a pH 7.4 PBS (50 mM) containing 100 mM NaCl, 5 mM $MgCl_2$.

2.6. Preparation of electrochemical cytosenor and electrochemical measurements

The gold electrode was cleaned first in Piranha solution (30% H_2O_2: 98% H_2SO_4 = 3:7, V/V) for 5 min twice and rinsed with water prior to use. (Safety note: the Piranha solution should be handled with carefully caution). All the oligonucleotides solutions were heat-treated in 90 °C for 3 min and then cooled in ice for 10 min before use.

For the preparation of electrochemical cytosensor, 20 μL of a thiolated-cDNA solution (5 μM) in phosphate buffer was first spread at the pre-cleaned gold electrode for 12 h at 37 °C in the 100% humidity. Then the electrode was blocked with 6-mercapto-1-hexanol (MCH) (1 mM, 100 μL) for 1 h. Next, it was covered with 20 μL aptamer solution (5 μM) and incubated for 1 h at 37 °C in 100% humidity to hybridize with cDNA on the electrode. At last,

10 μL of carboxylic group functionalized CdTe Qdots activated with EDC and NHS were dropped onto the electrode surface to conjugate with 5′-NH_2-modified aptamer. Then tween-20 was used to remove the unbonded Qdots. After each self-assemble step, the electrode was thoroughly washed with water and dried with N_2 stream. The obtained Qdots/Apt/cDNA/Au electrode was used for the subsequent assay.

For competitive binding, 10 μL of desired amount of cells was added to the fabricated electrode and incubated for 30 min at 37 °C, 5% CO_2. Then the electrode was thoroughly rinsed with deionized water and dried with N_2 stream. After the competitive binding, the gold electrode was immersed in 100 μL of 0.1 M HNO_3 for 2 h to dissolve the residual Qdots. Subsequently, the above dissolution solution (100 μL) was added into a glass cell containing 1.9 mL acetate buffer (0.2 M, pH 5.2) spiked with 10 ppm mercury (II). The SWASV detection involved pretreatment at +0.6 V for 1 min, and electrodeposition at −1.1 V for 4 min, and stripping from −1.1 V to −0.2 V under N_2 atmosphere using a square-wave voltammetric waveform, with 4 mV potential steps, 25 Hz frequency and 25 mV amplitude [30].

2.7. Cell lines and cell culture

MCF-7 cells (human Breast adenocarcinoma), HeLa cells (human Cervix adenocarcinoma) and HL-60 cells (human Acute promyelocytic leukemia) were obtained from Nanjing KeyGen Biotech Co. Ltd. MCF-7 and HeLa cells were cultured in a flask in DMEM medium (Gibco, Grand Island, NY) supplemented with 10% fetal calf serum (FCS, Sigma), penicillin (100 μg mL^{-1}), and streptomycin (100 μg mL^{-1}) in an incubator (5% CO_2, 37 °C). The cells were collected from 90% confluent cell culture plates by aspirating off the media and incubating with trypsin for 3–5 min. Five milliliters of media was added to dilute and neutralize the trypsin solution. Then this solution was separated from the medium by centrifugation at 1000 rpm for 10 min and washed twice with a sterile PBS. The sediment was suspended in the PBS to obtain a homogeneous cell suspension with the final concentration of ~10^7 cells mL^{-1}. The cell density was determined by using a Petroff-Hausser cell counter (USA) and this was performed prior to the experiments. The cell suspensions with various contents were prepared from this stock. HL-60 cells were cultured in a flask in RPMI 1640 medium (Gibco, Grand Island, NY) supplemented with the same as other cells.

2.8. Specific recognition of Apt-Qdots conjugates to MCF-7 cells

To demonstrate the targeting capabilities of Apt-Qdots conjugates toward MCF-7 cells, fluorescence imaging was observed by a confocal microscope. The binding was performed by the following procedure. Approximately, 5×10^6 cells mL^{-1} was obtained in test tubes. Then, 50 μL of Apt-Qdots conjugates were added into the cell sample and incubated at 37 °C, 5% CO_2 for 30 min. After incubation, the cells were washed twice by centrifugation with a sterile PBS and resuspended in 20 μL of buffer. In order to demonstrate the detected fluorescence signal came from the specific binding of Apt-Qdots with MUC1 on the surface of MCF-7 cells, two control experiments were conducted. The cell samples were first incubated with aptamer alone for 30 min and then with Apt-Qdots conjugates for another 30 min. The other experiment was carried out using Qdots to incubate with cells directly. All other procedures were the same with the former.

2.9. Cell imaging

10 μL of cell suspension bound with Apt-Qdots conjugates was dropped on a thin glass slide and covered with a coverslip. Then the glass slide was inverted and placed above a 40× objective on the confocal microscope. Fluorescence imaging was conducted with a confocal microscope (TCS SP5, Leica, Germany). The CdTe Qdots were excited with 488 nm laser line and detected with 550–650 nm band-pass filter.

3. Results and discussion

3.1. Characterization of the CdTe Qdots and Apt-Qdots conjugates

The photoluminescence (PL) and absorption spectra of the CdTe Qdots colloid solution were shown in Fig. 1. The PL emission peak and the absorption peak appeared at 630 nm and 550 nm, respectively. It could be seen that the line width of PL spectrum was very narrow and symmetric, indicating the Qdots were nearly monodisperse and homogeneous. The particle size was estimated to be 4.1 nm from the first absorption peak wavelength [54].

After CdTe was conjugated with aptamer, its properties changed obviously, indicating the formation of the Apt-Qdots conjugates. The PL, UV–vis and FT-IR absorption spectra were used to characterize these changes. As shown in Fig. 2A, about 5 nm blue-shift in the PL emission peak was observed after the Qdots conjugated with aptamer. This might be ascribed to the energy-transfer by selective Qdots luminescence quenching and light scattering [56]. And the UV absorption peak of aptamer at 260 nm could be obtained in Apt-Qdots conjugates (inset in Fig. 2A). FT-IR spectrum could also testify the successful fabrication of the conjugation. As shown in Fig. 2B, the characteristic absorption peak of DNA at 1650, 1080 and 980 cm^{-1} were preserved after the formation of Apt-Qdots conjugates [57].

3.2. Construction of cytosensor by electrochemical methods

Electrochemical Impedance spectroscopy (EIS) is a powerful tool for monitoring the changes of interfacial properties on electrode surface [58]. Nyquist plot of EIS measurement shows a semicircle in the high-frequency region associated with resistance and capacitance and a straight line in the low-frequency region associated with mass transfer. The semicircle diameters correspond to the electro-transfer resistance (R_{et}). Herein, EIS was used to characterize the fabrication procedure and significant differences in the EIS were observed during the modification. The bare gold electrode displayed an almost straight line (curve a in Fig. 3A) indicating a fast electron-transfer process of $Fe(CN)_6^{3-/4-}$. The immobilization of 5′-thiol-modified cDNA on the gold electrode surface through Au–SH bond led to an enhanced electron-transfer resistance (R_{et} = 4.5 KΩ, curve b in Fig. 3A), mainly due to the electrostatic repulsion between negative charges of the cDNA backbone and the $Fe(CN)_6^{3-/4-}$ probe. This demonstrated that cDNA was assembled onto the electrode. After aptamer hybridized with cDNA, a further increase in R_{et} (from 4.5 KΩ to 6 KΩ, curve c in Fig. 3A) could be observed, because negatively charged aptamer could repel the negative charged redox probe $Fe(CN)_6^{3-/4-}$ and thus the interfacial electron transfer resistance was increased [59–61]. Then the carboxylated CdTe Qdots activated with EDC and NHS were dropped on the electrode surface and covalently linked to 5′-NH_2 modified aptamer, which resulted in an increased electron transfer resistance (R_{et} = 9.5 KΩ, curve d in Fig. 3A). Such resistance increase could be attributed to the fact that CdTe Qdots carried negative charges in pH 7.4 PBS, as their zeta potential peak was at -48.2 mV. Afterward, the Qdots/Apt/cDNA/Au modified electrode was incubated with MCF-7 cells and a competition took place between MCF-7 cells and cDNA to bind with Apt-Qdots conjugates, leading to a significant decrease of R_{et} (from 9.5 KΩ to 8 KΩ, curve e in Fig. 3A). When the Qdots left on the electrode surface were dissolved by HNO_3, the electrical impedance further decreased (R_{et} = 7 KΩ, curve

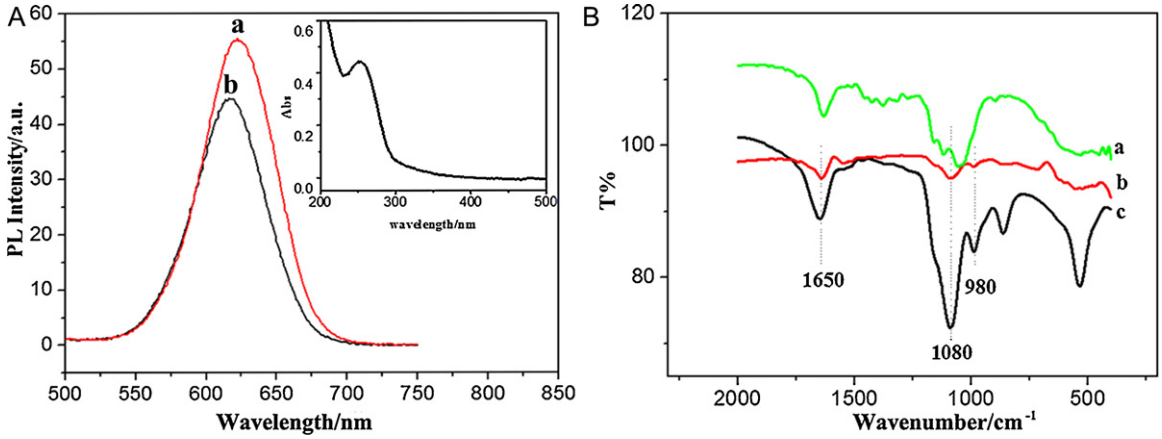

Fig. 2. (A) PL spectra of Qdots (a) and Apt-Qdots conjugates (b). Inset: UV–vis absorption spectrum of Apt-Qdots conjugates. (B) FTIR spectra of pure Qdots, (a) Apt-Qdots conjugates (b) and pure aptamer (c).

f in Fig. 3A). The EIS results indicated that the immobilization, competitive binding and resolving were accomplished as expected.

Cyclic voltammetry was also used to characterize the modified electrode after each assembly step with the redox probe of $Fe(CN)_6^{3-/4-}$. As shown in Fig. 3B, a pair of well-defined redox peak was observed at bare gold electrode (curve a), showing the excellent electron-transfer kinetics of $Fe(CN)_6^{3-/4-}$. After the electrode was assembled with cDNA and MCH, the peak to peak potential separation increased greatly and the amperometric response decreased (curve b), indicating increased irreversibility of the interfacial electron transfer. When aptamer and Qdots were combined to the gold electrode surface, similar phenomena were obtained (curve c and d). However, upon incubated with MCF-7 cells, the competitive reaction took place and only a few Apt-Qdots were left on the electrode surface, which resulted in the peak current increase (curve e). After dissolving the remaining Qdots by HNO_3, the peak current further increased (curve f). The CV behaviors accorded with the EIS changes, which further confirmed the successful modification and expected competition.

3.3. Optimization of cDNA and aptamer amount

With the increasing of cDNA and aptamer at the modified electrode, the stripping peak current increased and then approached a constant value. In order to obtain the optimum conditions, cDNA concentration was firstly considered. With the increasing amount of cDNA, the Ret of gold electrode increased gradually and reached a steady state eventually as shown in Fig. 4A. This illustrated that more cDNA could be immobilized on the gold electrode surface and reached saturated binding at the amount of 15 μL (5 μM). We chose 20 μL (5 μM) of the solution to ensure a complete saturated binding in the following experiments. On the other hand, the influence of aptamer concentration on the stripping peak current was also investigated and the optimum concentration of aptamer was 20 μL (5 μM) (Fig. 4B).

3.4. Competition assay for cell detection

In our assay, the electrochemical signal was directly related to the amount of cells which were used to compete with cDNA at the electrode. With the increasing of cells, the number of Qdots left at the electrode decreased. The peak current was inversely proportional to the logarithmic value of cell concentration ranging from 1.0×10^2 to 1.0×10^6 cells mL^{-1} with a correlation coefficient R of 0.9931 ($n = 6$) (Fig. 5) and the detection limit was 100 cells mL^{-1} which was comparable to those reported by most of aptamer-based assays [62] and other electrochemical and fluorescence cytosensing strategy for cancer cell detection [20,63–65]. We should mention

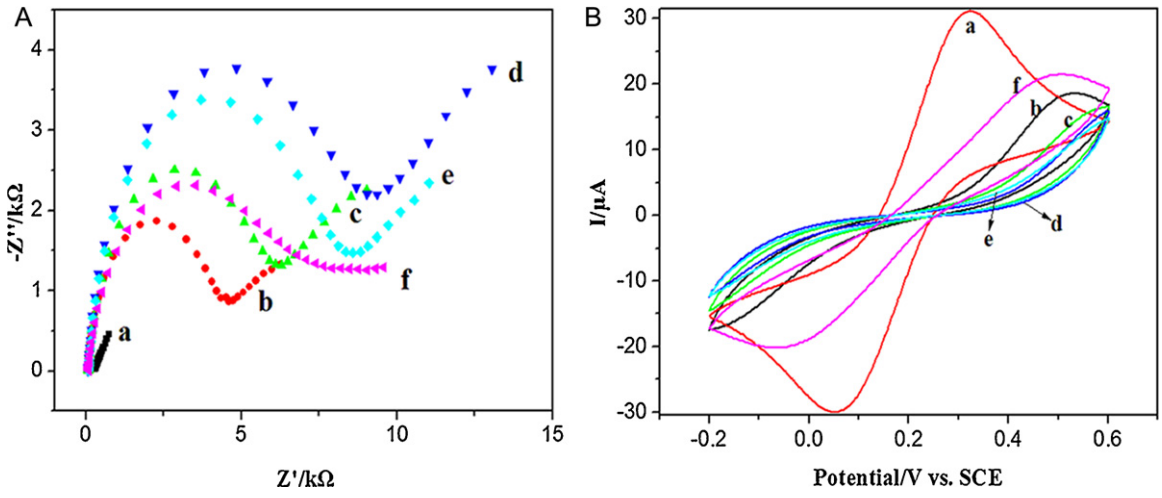

Fig. 3. (A) Nyquist diagrams of electrochemical impedance spectra recorded from 0.1 to 10^5 Hz for $[Fe(CN)_6]^{3-}/[Fe(CN)_6]^{4-}$ (10 mM, 1:1) in 0.1 M KCl. (B) Cyclic Voltammograms at a bare Au electrode (a), cDNA/Au electrode (b), Apt/cDNA/Au electrode (c), Qdots/Apt/cDNA/Au electrode (d), MCF-7/Qdots/Apt/cDNA/Au electrode (e) and the final electrode after HNO_3 dissolving (f).

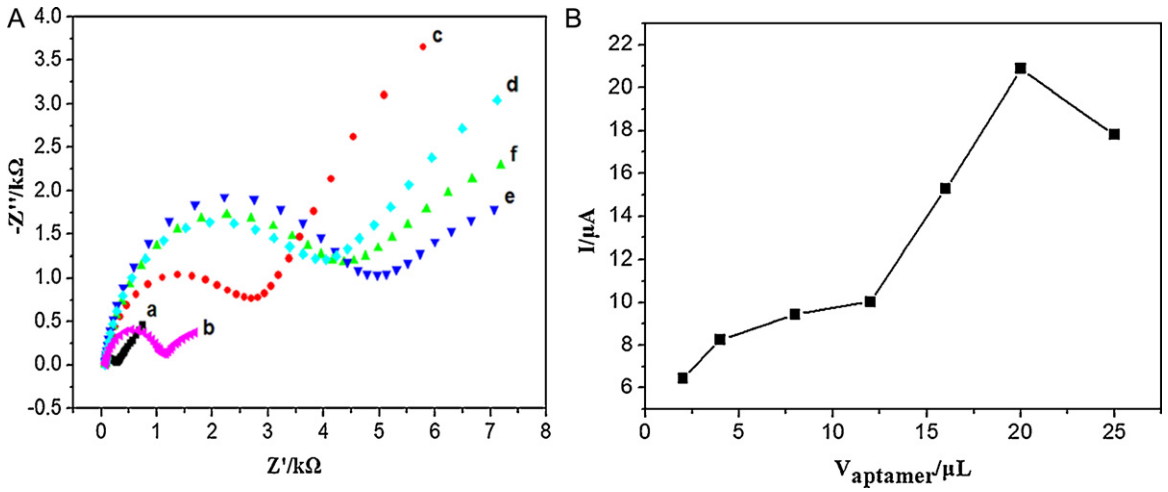

Fig. 4. (A) Nyquist diagrams of electrochemical impedance spectra recorded from 0.1 to 10^5 Hz for $[Fe(CN)_6]^{3-}/[Fe(CN)_6]^{4-}$ (10 mM, 1:1) in 0.1 M KCl at a bare Au electrode (a), cDNA/Au electrode with the cDNA amount of 5, 10, 15, 20, 30 μL (from curve b–f). (B) Effect of aptamer amount in electrode modification on peak current of Qdots/Apt/cDNA/Au electrode.

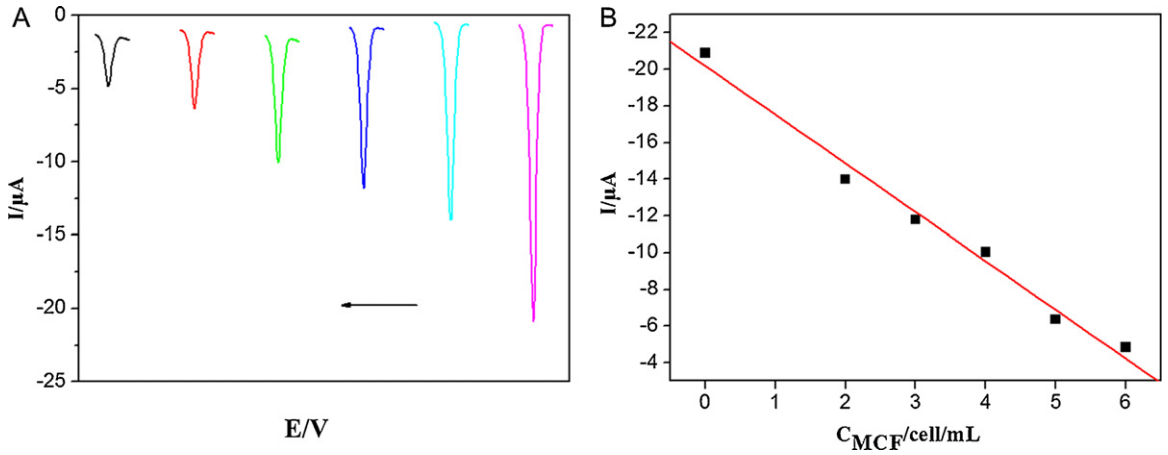

Fig. 5. Competition between cells and cDNA for binding to Apt-Qdots conjugates. A) Anodic stripping voltammograms of Qdots left at the modified gold electrode competing with 0, 10^2, 10^3, 10^4, 10^5 and 10^6 cells mL^{-1} (right to left). B) The corresponding linear calibration plot.

that, above the number of cells indicated in the plot, the electrochemical response of this cytosensor began to plateau. At the cell concentration of 1.0×10^3 cells mL^{-1}, the cytosensor had the relative standard deviation of 2.3% examined for five determinations, showing good reproducibility.

The specificity of the cytosensor for MCF-7 cells was further studied. HeLa and HL-60 cells in place of MCF-7 cells were tested, using the same experimental procedures as those for MCF-7 cells. As shown in Fig. 6, compared with signal response of the cytosensor to MCF-7 cells, some changes were observed in the case of HeLa and HL-60 cells, which resulted from the MUC1 protein overexpressed [66]. However, such response could not affect the specificity of the cytosensor for the determination of MCF-7 cells and might be solved by multiplex biomarker detection [67]. Thus, the established competitive electrochemical cytosensor displayed a good performance for the detection of MCF-7 cancer cells with broad detection range, low detection limit, good reproducibility and specificity.

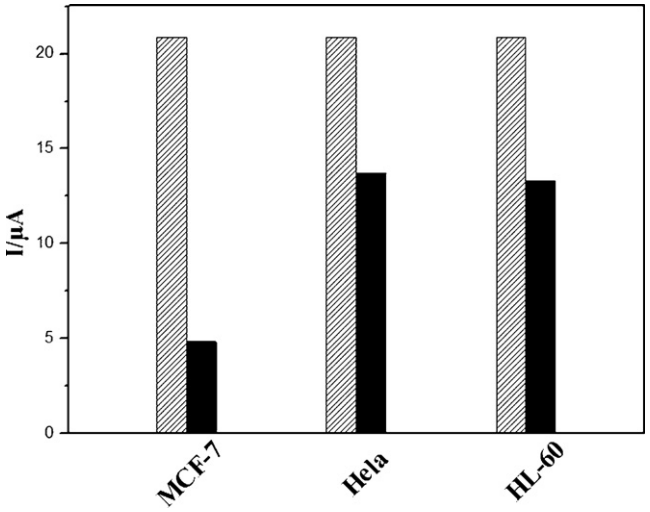

Fig. 6. Bar graph showed the change in peak current between the target cells and control cells, showing the specificity of the assay for the target cells. The concentration of cells were all 1.0×10^6 cells mL^{-1}.

3.5. Confocal imaging of Apt-Qdots conjugate specific bound with MCF-7 cells

In our proposed assay, Qdots were not only used to read out detection signal, but also served as the fluorescence probe to

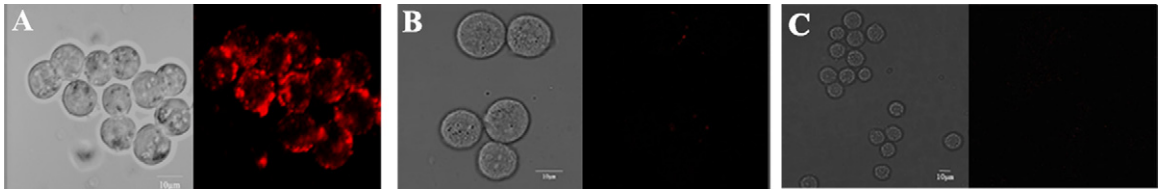

Fig. 7. Confocal studies of specific recognition of Apt-Qdots conjugates to MCF-7 cells. Apt-Qdots conjugates labeling of MCF-7 cells (A); Fluorescence images of MCF-7 cells after reacted with aptamer for 30 min and then with Apt-Qdots conjugates for another 30 min (B) and MCF-7 cells reacted with CdTe Qdots only (C).

visualize the specific binding between Apt-Qdots conjugates and the target cells. Fluorescence confocal imaging was used here for this purpose. In order to demonstrate that the Apt-Qdots conjugates could bind with the target cells, Apt-Qdots conjugates were incubated with MCF-7 for 30 min at 37 °C. Fig. 7A showed the Qdots fluorescence on MCF-7 cells obviously, suggesting that the Apt-Qdots conjugates could effectively bind with these cells.

To further prove that the detected fluorescence signal was originated from the specific binding of Apt-Qdots conjugates with the target cells, two control experiments were carried out. The cell samples were first incubated with aptamer alone for 30 min and then with Apt-Qdots conjugates for another 30 min. The fluorescence signal could hardly be detected as shown in Fig. 7B. It is because that the cells were first conjugated with free aptamer before the addition of Apt-Qdots conjugate which led to occupation of the MUC1 sites and prevented subsequent binding of the Apt-Qdots conjugates [6]. It indicated that the combination between Apt-Qdots and MCF-7 cells came from the recognition ability of aptamer to MUC1 protein. The other control experiments used Qdots to incubate with MCF-7 cells directly and no obvious fluorescence was detected in the cells as shown in Fig. 7C. Thus, the obtained fluorescence emission in Fig. 7A resulted from the specific binding between Apt-Qdots conjugates and MCF-7 cells without non-specific absorption of Qdots on the cell surface.

4. Conclusions

A novel electrochemical cytosenor for the detection of tumor cells was developed based on the competitive reaction between the target protein and the cDNA. Aptamer-Qdot conjugates were used to establish an efficient and intuitionistic dual-stage platform for the cancer cell detection and recognition. This was realized by the characteristics as follows: (i) the high selectivity of aptamer; (ii) the metal species of QDots; and (iii) well fluorescence emission properties of Qdots. To the best of knowledge, it is the first time that Apt-Qdots conjugates have been used for the fabrication of electrochemical cytosensor to detect cancer cells. The high sensitity will be useful for early diagnosis of cancer. All of the reactions occurred on the surface of gold electrode and there was no need for extra separation. Furthermore, this strategy can be easily extended to other cancer cells and analytes.

Acknowledgements

This study was supported by the National Natural Science Foundation of China (nos. 50972058, 21005034, 20821063) and National Basic Research Program of China (2011CB933502).

References

[1] J.J. Zhang, M.M. Gu, T.T. Zheng, J.J. Zhu, Anal. Chem. 81 (2009) 6641–6648.
[2] C. Hao, L. Ding, X.J. Zhang, H.X. Ju, Anal. Chem. 79 (2007) 4442–4447.
[3] Q. Shen, S.K. You, S.G. Park, H. Jiang, D.D. Guo, B.A. Chen, X.M. Wang, Electroanalysis 20 (2008) 2526–2530.
[4] W. Cheng, L. Ding, S.J. Ding, Y.B. Yin, H.X. Ju, Angew. Chem. Int. Ed. 48 (2009) 6465–6468.
[5] D.E. Woolley, L.C. Tetlow, D.J. Adlam, D. Gearey, R.D. Eden, Biotechnol. Bioeng. 77 (2002) 725–733.
[6] L. Ding, W. Cheng, X.J. Wang, S.J. Ding, H.X. Ju, J. Am. Chem. Soc. 130 (2008) 7224–7225.
[7] A.D. Ellington, J.W. Szostak, Nature 346 (1990) 818–822.
[8] A.D. Ellington, J.W. Szostak, Nature 355 (1992) 850–852.
[9] C. Tuerk, L. Gold, Science 249 (1990) 505–510.
[10] C.H. Lin, D. Patel, J. Chem. Biol. 4 (1997) 817–832.
[11] W.A. Zhao, W. Chiuman, J.C.F. Lam, S.A. Mcmanus, W. Chen, Y.G. Cui, R. Pelton, M.A. Brook, Y.F. Li, J. Am. Chem. Soc. 130 (2008) 3610–3618.
[12] D. Zheng, D.S. Seferos, D.A. Giljohann, P.C. Patel, C.A. Mirkin, Nano Lett. 9 (2009) 3258–3261.
[13] A. Higuchi, Y.D. Siao, S.T. Yang, P.V. Hsieh, H. Fukushima, Y. Chang, R.C. Ruaan, W.Y. Chen, Anal. Chem. 80 (2008) 6580–6586.
[14] K. Yan, K.J. Feng, J.W. Chen, J.H. Jiang, G.L. Shen, R.Q. Yu, Bioelectrochemistry 73 (2008) 76–81.
[15] M. Mir, A.T.A. Jenkins, I. Katakis, Electrochem. Commun. 10 (2008) 1533–1536.
[16] D.H. Shangguan, Y. Li, Z.W. Tang, Z.H.C. Cao, H.W. Chen, P. Mallikaratchy, K. Sefah, C.Y.J. Yang, W.H. Tan, Proc. Natl. Acad. Sci. U.S.A. 103 (2006) 11838–11843.
[17] C.L.A. Hamula, H.Q. Zhang, L.L. Guan, X.F. Li, X.C. Le, Anal. Chem. 80 (2008) 7812–7819.
[18] M.C. Rebeca, D.L.S.A. Noemi, J.L.C. Maria, J.M.O. Arturo, T.B. Paulino, Electroanalysis 21 (2009) 2077–2090.
[19] H. Wang, R.H. Yang, L. Yang, W.H. Tan, ACS Nano 3 (2009) 2451–2460.
[20] J.E. Smith, C.D. Medley, Z.W. Tang, D.H. Shangguan, C. Lofton, W.H. Tan, Anal. Chem. 79 (2007) 3075–3082.
[21] J.H. Choi, K.H. Chen, J.H. Han, A.M. Chaffee, M.S. Strano, Small 5 (2009) 672–675.
[22] I. Willner, M. Zayats, Angew. Chem. Int. Ed. 46 (2007) 6408–6418.
[23] H.P. Huang, G.F. Jie, R.J. Cui, J.J. Zhu, Electrochem. Commun. 11 (2009) 816–818.
[24] K.J. Feng, Y. Kang, J.J. Zhao, Y.L. Liu, J.H. Jiang, G.L. Shen, R.Q. Yu, Anal. Biochem. 378 (2008) 38–42.
[25] B.R. Baker, R.Y. Lai, M.S. Wood, E.H. Doctor, A.J. Heeger, K.W. Plaxco, J. Am. Chem. Soc. 128 (2006) 3138–3139.
[26] J.W. Liu, Z.H. Cao, Y. Lu, Chem. Rev. 109 (2009) 1948–1998.
[27] E.E. Ferapontova, E.M. Olsen, K.V. Gothelf, J. Am. Chem. Soc. 130 (2008) 4256–4258.
[28] A. Numnuam, K.Y. Chumbimuni-Torres, Y. Xiang, R. Bash, P. Thavarungkul, P. Kanatharana, E. Pretsch, J. Wang, E. Bakker, Anal. Chem. 80 (2008) 707–712.
[29] D.D. Shen, H.L. Zhang, Q. Qi, F. Gao, C.X. Ma, Zhang, Biosens. Bioelectron. 23 (2008) 1624–1630.
[30] J.A. Hansen, J. Wang, A.N. Kawde, Y. Xiang, K.V. Gothelf, G. Collins, J. Am. Chem. Soc. 128 (2006) 2228–2229.
[31] Y. Huang, X.M. Nie, S.L. Gan, J.H. Jiang, G.L. Shen, R.Q. Yu, Anal. Biochem. 382 (2008) 16–22.
[32] J. Wang, Small 1 (2005) 1036–1043.
[33] M. Bruchez Jr., M. Moronne, P. Gin, S. Weiss, A.P. Alivisatos, Science 281 (1998) 2013–2016.
[34] W.C.W. Chan, S.M. Nie, Science 281 (1998) 2016–2018.
[35] C. Walther, K. Meyer, R. Rennert, I. Neundorf, Bioconjugate Chem. 19 (2008) 2346–2356.
[36] V. Bagalkot, L.F. Zhang, E. Levy-Nissenbaum, S.Y. Jon, P.W. Kantoff, R. Langer, O.C. Farokhzad, Nano Lett. 7 (2007) 3065–3070.
[37] X.C. Chen, Y.L. Deng, Y. Lin, D.W. Pang, H. Qing, F. Qu, H.Y. Xie, Nanotechnology 19 (2008) 235105–235111.
[38] T.C. Chu, F. Shieh, L.A. Lavery, M. Levy, R. Richards-Kortum, B.A. Korgel, A.D. Ellington, Biosens. Bioelectron. 21 (2006) 1859–1866.
[39] J. Zhang, X. Jia, X.J. Lv, Y.L. Deng, H.Y. Xie, Talanta 81 (2010) 505–509.
[40] Z.H. Cao, R. Tong, A. Mishra, W.C. Xu, G.C.L. Wong, J.J. Cheng, Y. Lu, Angew. Chem. Int. Ed 48 (2009) 6494–6498.
[41] J.L. He, Z.S. Wu, S.B. Zhang, G.L. Shen, R.Q. Yu, Talanta 80 (2010) 1264–1268.
[42] C.S.M. Ferreira, C.S. Matthews, S. Missailidis, Tumor Biol. 27 (2006) 289–301.
[43] S. von Mensdorff-Pouilly, F.G.M. Snijdewint, A.A. Verstraeten, R.H. Verheijen, P. Kenemans, Int. J. Biol. Markers 15 (2000) 343–356.
[44] S.J. Gendler, J Mammary Gland Biol. Neoplasia 6 (2001) 339–353.
[45] C.D. Pieve, A.C. Perkins, S. Missailidis, Nucl. Med. Biol. 36 (2009) 703–710.
[46] C.S.M. Ferreira, K. Papamichael, G. Guilbault, T. Schwarzacher, J. Gariepy, S. Missailidis, Anal. Bioanal. Chem. 390 (2008) 1039–1050.
[47] K.E. Borbas, C.S.M. Ferreira, A. Perkins, J.I. Bruce, S. Missailidis, Bioconjugate Chem. 18 (2007) 1205–1212.
[48] A.K.H. Cheng, H.P. Su, Y.A. Wang, H.Z. Yu, Anal. Chem. 81 (2009) 6130–6139.
[49] L. Gold, D. Ayers, J. Bertino, C. Bock, A. Bock, et al., PLOS ONE 5 (2010) e15004.

[50] H.F. Qian, C.Q. Dong, J.F. Weng, J.C. Ren, Small 2 (2006) 747–751.
[51] H. Zhang, D.Y. Wang, B. Yang, H. Möhwald, J. Am. Chem. Soc. 128 (2006) 10171–10180.
[52] R.J. Cui, H.C. Pan, J.J. Zhu, H.Y. Chen, Anal. Chem. 79 (2007) 8494–8501.
[53] Z. Zhelev, R. Bakalova, H. Ohba, R. Jose, Y. Imai, Y. Baba, Anal. Chem. 78 (2006) 321–330.
[54] W.W. Yu, L.H. Qu, W.Z. Guo, X.G. Peng, Chem. Mater. 15 (2003) 2854–2860.
[55] J. Wang, G.D. Liu, A. Merkoci, J. Am. Chem. Soc. 125 (2003) 3214–3215.
[56] J. Riegler, F. Ditengou, K. Palme, T. Nann, J. Nanobiotechnol. 6 (2008) 7–12.
[57] T.B. Yang, B.C. Zhu, L.B. Li, J. Hebei Univ. (Nat. Sci. Ed.) 11 (1991) 35–42.
[58] S.M. Park, J.S. Yoo, Anal. Chem. 75 (2003) 455A–461A.
[59] A.E. Radi, J.L.A. Sánchez, E. Baldrich, C.K. O'Sullivan, Anal. Chem. 77 (2005) 6320–6323.
[60] M. Zayats, Y. Huang, R. Gill, C.A. Ma, I. Willner, J. Am. Chem. Soc. 128 (2006) 13666–13667.
[61] N. de-los-Santos-Álvarez, M.J. Lobo-Castañón, A.J. Miranda-Ordieres, P. Tuñón-Blanco, J. Am. Chem. Soc. 129 (2007) 3808–3809.
[62] C.F. Pan, M. Guo, Z. Nie, X.L. Xiao, S.Z. Yao, Electroanalysis 21 (2009) 1321–1326.
[63] M. Xie, J. Hu, Y.M. Long, Z.L. Zhang, H.Y. Xie, D.W. Pang, Biosens. Bioelectron. 24 (2009) 1311–1317.
[64] C.D. Medley, J.E. Smith, Z.W. Tang, Y.R. Wu, S. Bamrungsap, W.H. Tan, Anal. Chem. 80 (2008) 1067–1072.
[65] X.R. Zhang, S.G. Li, X. Jin, X.M. Li, Biosens. Bioelectron. 26 (2011) 3674–3678.
[66] N. Li, J.N. Ebright, G.M. Stovall, X. Chen, H.H. Nguyen, A. Singh, A. Syrett, A.D. Ellington, J. Proteome Res. 8 (2009) 2438–2448.
[67] W.J. Kang, J.R. Chae, Y.L. Cho, J.D. Lee, S. Kim, Small 5 (2009) 2519–2522.